An advanced fabrication method of highly ordered ZnO nanowire arrays on silicon substrates by atomic layer deposition

2012 Nanotechnology 23 235607

(http://iopscience.iop.org/0957-4484/23/23/235607)

Nanotechnology **23** (2012) 235607 (7pp) doi:10.1088/0957-4484/23/23/235607

An advanced fabrication method of highly ordered ZnO nanowire arrays on silicon substrates by atomic layer deposition

Kittitat Subannajui[1,2], Firat Güder[1,4], Julia Danhof[3,4], Andreas Menzel[1,4], Yang Yang[1], Lutz Kirste[3], Chunyu Wang[3], Volker Cimalla[3], Ulrich Schwarz[3] and Margit Zacharias[1]

[1] Institute of Microsystems Engineering, University of Freiburg, Georges Koehler Allee 103, 79110 Freiburg, Germany
[2] Mahidol University, 272 Rama VI Road, Ratchathewi District, Bangkok 10400, Thailand
[3] Fraunhofer Institute for Applied Solid State Physics, Tullastraße. 72, 79108 Freiburg, Germany

E-mail: kittitat.subannajui@imtek.uni-freiburg.de

Received 30 January 2012, in final form 24 April 2012
Published 18 May 2012
Online at stacks.iop.org/Nano/23/235607

Abstract
In this work, the controlled fabrication of highly ordered ZnO nanowire (NW) arrays on silicon substrates is reported. Si NWs fabricated by a combination of phase shift lithography and etching are used as a template and are subsequently substituted by ZnO NWs with a dry etching technique and atomic layer deposition. This fabrication technique allows the vertical ZnO NWs to be fabricated on 4 in Si wafers. Room temperature photoluminescence and micro-photoluminescence are used to observe the optical properties of the atomic layer deposition (ALD) based ZnO NWs. The sharp UV luminescence observed from the ALD ZnO NWs is unexpected for the polycrystalline nanostructure. Surprisingly, the defect related luminescence is much decreased compared to an ALD ZnO film deposited at the same time on a plane substrate. Electrical characterization was carried out by using nanomanipulators. With the p-type Si substrate and the n-type ZnO NWs the nanodevices represent p–n NW diodes. The nanowire diodes show a very high breakthrough potential which implies that the ALD ZnO NWs can be used for future electronic applications.

S Online supplementary data available from stacks.iop.org/Nano/23/235607/mmedia

(Some figures may appear in colour only in the online journal)

1. Introduction

ZnO nanowires (NWs), as one of the easiest grown materials for semiconductor nanowires, have been intensively studied in the past [1]. Their physical properties as well as applications have been extensively investigated [2–4] with the high aspect ratio of the nanowire structure being an advantage for special properties of future electronic devices such as, for example, luminescence devices, biological sensors, and gas sensors [4–6]. In a real large scale electronic production, an integration of ZnO nanostructures and microsystem technology is usually required. However, many fabrication routes for ZnO NWs require temperatures as high as 900 °C, and the ZnO NWs are grown randomly, densely and even interlinked as a forest like structure which is often unsuitable for electronic applications [7]. An integration of high temperature processes with microelectronic devices could damage other microstructures, enhance unwanted diffusion processes and defects and consume a large amount of fabrication energy. Therefore, a low temperature process is a more suitable method in terms of production efficiency, and new reliable low temperature fabrication processes are

[4] These authors made large contributions to this paper.

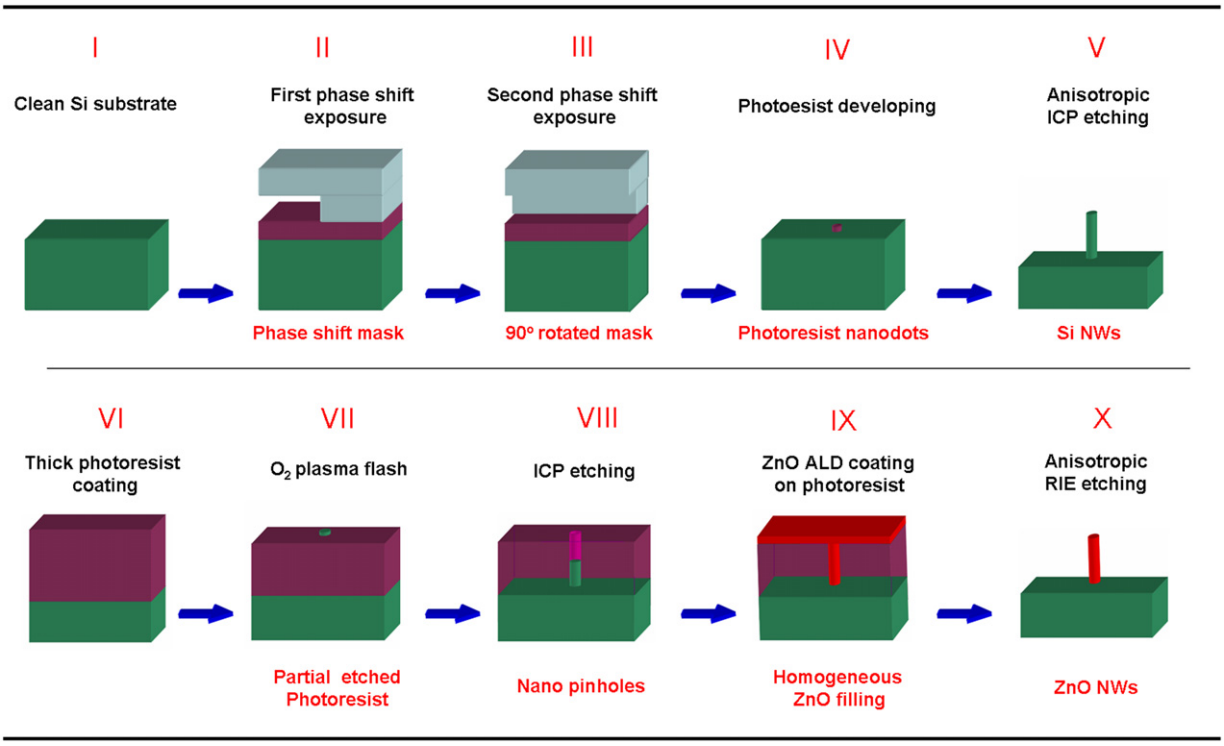

Figure 1. The fabrication process of the ALD ZnO NWs.

needed. In our recent work, a nanodot pattern fabricated by phase shift lithography on the wafer scale was reported [8]. In this work, a Si substrate, which is one of the most common substrate materials in microelectronics and microsystems engineering, was used. The success of nanowire fabrication in this work yields a strong potential in nano- and microsystem technology integration. The photoresist nanodots were etched and vertically aligned Si NWs were obtained as a result. In the paper presented here, we demonstrate how the Si NWs can be used in a template like way to fabricate ZnO NWs on a wafer scale with an extremely clean and low temperature route.

2. Experimental processes

The fabrication method started with the preparation of a clean Si surface (figure 1(I)). After an RCA cleaning process, near field phase shift lithography (NF-PSL) was carried out on a 4 in wafer. The density of Si NWs and ZnO NWs could be designed by the master mask which was used to fabricate the phase shift lithography mask [8]. In figure 1(II) the phase shift mask was placed on top of the photoresist, and the Si wafer was exposed to UV. After the first exposure, the phase shift mask was rotated by 90 ° and the second exposure was performed. Only at the intersection of the two exposures was a critical dose reached, establishing the desired pattern as shown in figure 1(III). After developing the photoresist, a wafer scale array of photoresist nanodots could be seen on the flat Si surface (figure 1(IV)). The Si wafer was then anisotropically etched by inductive coupled plasma (ICP) and an ordered array of etched Si NWs was obtained. The diameter of Si NWs depends mainly on the diameter of photoresist nanodots which can be controlled by the type of photoresist, exposure time, and developing time. The length of the Si NWs can be controlled by the ICP process. The longer the ICP process time is, the longer the Si NWs are. In this paper, the length of the Si NWs was kept at 1 μm. Figure 1(V) shows the Si NWs on the Si substrate after the ICP etching process. These etched Si NWs can now be used as a template. In figure 1(VI), a thick photoresist was spun onto the Si wafer embedding all the Si NWs inside it. The photoresist was then partially etched by O_2 plasma until the tops of the Si NWs towered slightly out of the surface of the photoresist layer (figure 1(VI)). After that the sample was again etched by ICP with the resist homogeneously covering the entire Si wafer except the tops of the Si NWs. Hence, only the Si NWs were etched away resulting in an ordered array of nano-pinholes (figure 1(VIII)). We now deposited ZnO by atomic layer deposition (ALD) with temperatures as low as 115 °C to fill the nano-pinholes. In addition to the low process temperature (115 °C), a main advantage of ALD is the deep and homogeneous penetration of the precursor molecules into high-aspect-ratio trenches and even μm deep nanopores (figure 1(IX)). The ALD ZnO film on top of the photoresist is later etched away by reactive ion etching (RIE), but the ZnO pillars still remain due to the high aspect ratio of the ZnO pillars as shown in figure 1(X). The last step is the same as typical spacer lithography which is normally used for low dimension nanostructure [9]. The obtained ALD ZnO NWs have diameters comparable to the grown ZnO NWs. Although the length of the ALD ZnO NWs was kept at 1 μm, it can be prolonged with a longer ICP process. Since the diameter of the ALD ZnO NWs was around 100 nm, the aspect ratio of the ALD ZnO NWs was 1:10. With

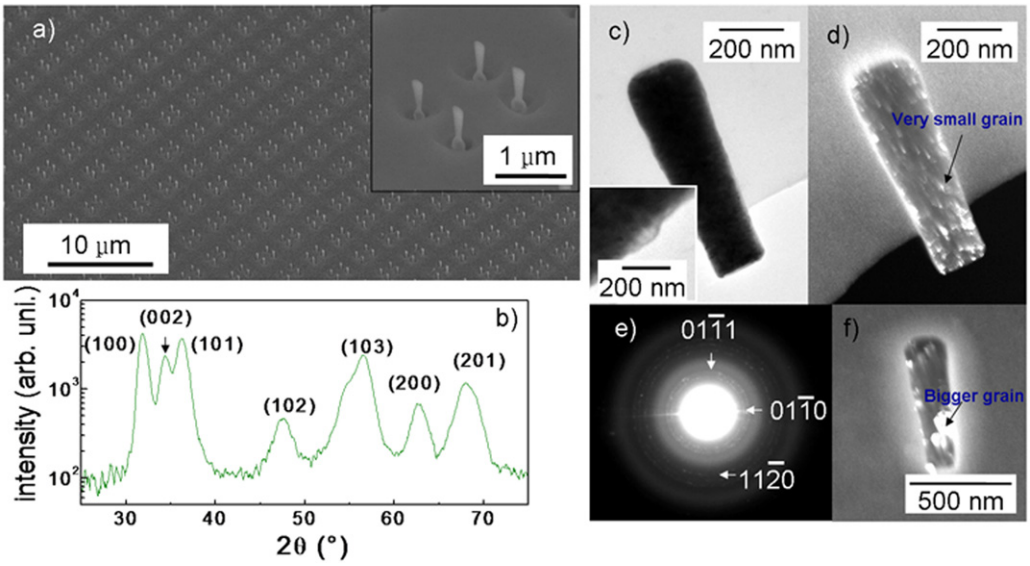

Figure 2. (a) A wafer scale array of ZnO NWs on a (100) Si wafer, and (inset) ALD ZnO NWs with an overetched surface. (b) XRD pattern of an ALD ZnO film with the same deposition batch as the ALD ZnO NWs. (c) Bright field TEM image of an ALD ZnO NW. The inset shows the remnant photoresist layer on the ZnO NW surface. (d) Dark field TEM image of the ALD ZnO NW. The ZnO NW is composed of many small ZnO grains. (e) The electron diffraction pattern of the ALD ZnO NW shown in (c). This ZnO nanowire is polycrystalline consisting of many crystal orientations. (f) Dark field TEM image of an ALD ZnO NW after annealing at 800 °C. The ZnO grains become larger and the crystallinity is improved.

the here presented technique, any material can be fabricated as vertical nanowire arrays as long as it can be deposited by ALD, which is very useful for future nanofabrication.

TEM images of the ZnO NWs and the corresponding ED pattern were obtained by using a JEOL 1010 microscope at an accelerating voltage of 100 kV. The NWs were scratched from the Si substrate, dispersed in ethanol (analytically pure, 99.99%), dip-coated onto a copper grid coated with thin carbon film, and dried at room temperature.

Information about the optical properties of these samples was provided by photoluminescence (PL). Two different experimental methods were used. To get a general overview over the sample without paying special attention to single NWs, macroscopic PL was used. As the source of excitation we used the fourth harmonic of a neodymium YAG laser providing a wavelength of 266 nm. The spectral resolution of the monochromator was about 0.33 nm. To investigate single NWs, micro-PL was employed. We used a home built setup with a spatial resolution of about 300 nm and a spectral resolution of 0.16 nm was used. As the source of excitation an argon ion laser was used, operated at a wavelength of 334 nm. For both setups, the excitation density was variable.

3. Results and discussion

The ALD ZnO NWs can be grown at any position with a very large scale fabrication as shown in figure 2(a) because phase shift lithography and spacer lithography are not bound by the complicated crystal orientation, the limit of growth area, or homogeneity. The inset of figure 2(a) represents the same ALD ZnO NWs but with a higher resolution. Apparently, the shape of the ZnO NWs is not perfectly cylindrical. The observed cone shape might be the result of, for example, the imperfect etching of the Si NWs and a possible instability of the photoresist. Instability of the photoresist might also occur during the ALD growth and O_2 plasma processing which had a temperature of up to 220 °C, enough to slightly change the morphology of the nano-pinholes. The craters around the ZnO NWs are over etching areas by RIE. This over etching of ZnO occurred because no etch-stop layer was used. The positions of ZnO NWs are exactly the same as the ones of the nanodots from NF-PSL. The process allows a vertical growth of ZnO NWs with an exact position on commercial Si(100) substrates, substrates which are normally incompatible for vertical ZnO NW growth [10].

Figure 2(c) shows a bright field TEM image of an ALD ZnO NW. Apparently, the ZnO NW is dense without visible voids, indicating that the nano-pinholes in the photoresist layer were completely filled by ALD ZnO. Remnant photoresist at the nanowire surface can be observed in the inset of figure 2(c). This remnant photoresist cannot be easily removed because the initial ZnO monolayer during the first ALD cycle was chemically bonded to the photoresist. Accordingly, after the ALD ZnO NWs are released with the photoresist removal, a thin resist layer can remain on the nanowire surface and work as an encapsulation layer. In figure 2(d), the orientation contrast from the dark field TEM image clearly reveals that the ALD ZnO NW is composed of many small grains (5–20 nm). Such multigrains are common phenomena observed for ZnO ALD film deposition [11, 12]. The electron diffraction of this nanowire shown in figure 2(e) indicates the random crystal orientation inside the ALD ZnO NW [13]. However, the grain size of ALD ZnO NWs can be modified by heat treatment. For example, when annealed at 800 °C the grains are significantly enlarged as shown in

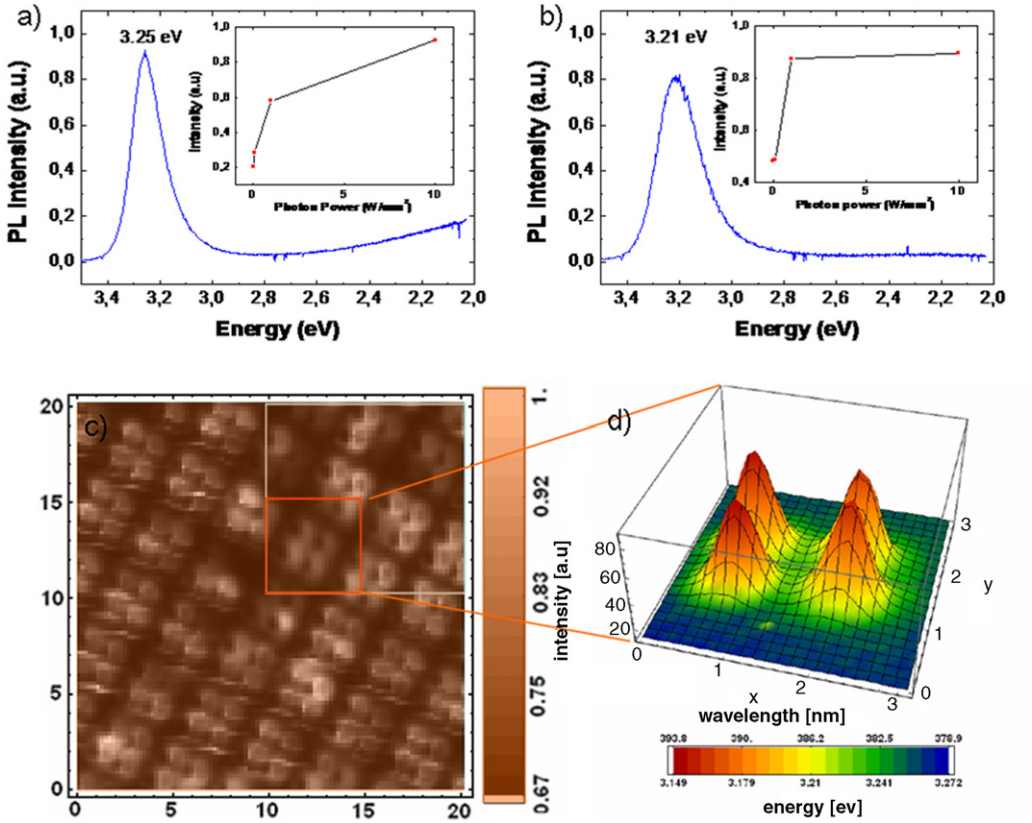

Figure 3. (a) Room temperature PL of the ALD ZnO film. The inset relates the laser power density with the UV intensities. (b) Room temperature PL of the ALD ZnO NWs, and (c) micro-PL intensities. The inset is the area used for the second investigation (d) with micro-PL at the positions of the ALD ZnO NWs.

figure 2(f). The growth of the grains inside the ALD ZnO NW is due to the Ostwald ripening which also improves the crystallinity in terms of reducing the total point defect density at the grain boundary [14].

We investigated the ALD ZnO NWs in comparison to the planar ALD ZnO film using room temperature photoluminescence (PL). In figure 3(a) the PL of the ALD ZnO film shows the near band edge peak (NBE) at 3.25 eV and a broad defect peak below 2.5 eV. The NBE intensity of the ALD ZnO film increases with higher laser power which means that the NBE exciton recombination was not yet saturated even at a laser power density of 10 W mm^{-2}. Figure 3(b) shows the PL from the ALD ZnO NWs using the same deposition conditions as for the ZnO film. A small red shift was observed for the ALD ZnO NWs compared to the PL observed from the ZnO film. The defect peak which exists in the case of the ALD ZnO film is drastically decreased in case of ALD ZnO NWs. The PL of the ALD grown ZnO NWs shows prominently only the NBE luminescence. The reason for the large reduction of the defect peak might be the surface passivation by remnant molecules from the photoresist. The remnant photoresist occurs from the bonding between the ALD ZnO molecules and the surface of the photoresist which can be observed in figure 2(c) (inset). Furthermore, the NBE intensity of the ALD ZnO NWs was observed to saturate already after the laser power density was increased to 1 W mm^{-2}. Such PL saturation was not found in the ALD ZnO film due to the lack of a surface passivation. Please note that the ALD ZnO NWs are well separated and hence the number of excited ZnO NWs is limited. We used micro-PL to analyze the ALD ZnO NWs. Figure 3(c) is a map of the integrated intensity. The spectra were integrated from 2.6 to 3.15 eV. The excitation density was about 900 W mm^{-2}. The areas in the white crop and red crop image shows the micro-PL emission intensities of repeated scans. These repeated scans were performed to obtain micro-PL maps of the sample with different resolutions. After the third repetition of the scan, the emission intensities decrease (within the red crop image). Since the structure, the laser power, and the emission energy are the same, the intensity of PL should not vary. We believe that this phenomenon occurred because of a surface charging effect. Figure 3(d) provides the three dimensional plot of one set of NWs. The x- and y-directions indicate the spatial position, the z-direction gives the intensity, and the emission energy is given in terms of color. The energy was obtained by calculating the first momentum of the spectra. For this scan, the excitation density was reduced to 450 W mm^{-2}. The sharp peaks of the NBE appear exactly at the positions of the ALD ZnO NWs which is a proof that the UV emission is coming from the ALD ZnO NWs. The PL results depict that the luminescence quality is good enough for optical applications such as nano-LEDs, even though the ALD ZnO NWs are not single crystals.

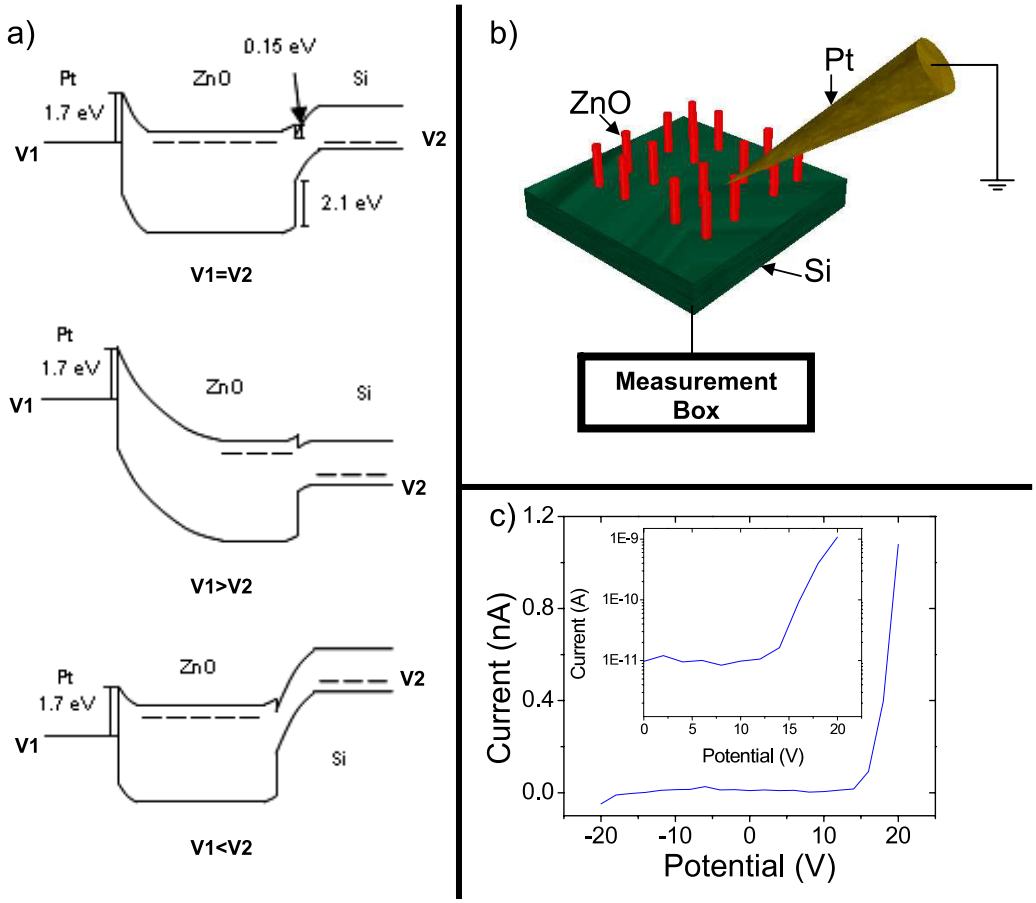

Figure 4. (a) The band diagram of Pt/n-ZnO/p-Si: without applied potential ($V1 = V2$), forward potential ($V1 > V2$), reverse potential ($V1 < V2$); (b) the measurement setup for the ALD ZnO NW diode; and (c) the I–V characteristic of the triple junction system; the inset shows the logarithmic scale for forward applied potentials.

Because we used a p-type Si substrate and the ALD ZnO NWs are of n-type, the resulting ALD ZnO NWs can be considered as an ordered array of nanowire diodes. In order to test the electrical properties of the ZnO NW diodes, a nanomanipulator was used to contact a free standing single nanowire. The tip of the manipulator was equipped with a sharp platinum (Pt) tip (figure 4(b)). However, when a Pt tip is used as a contact, the system becomes a triple material junction. The Si and ZnO form a diode junction, and the Pt and ZnO form a Schottky junction as shown in figure 4(a) ($V1 = V2$). In this system, there is a large hole barrier at the p–n junction which blocks the holes from transporting through the p–n junction. The holes have to overcome the barrier and the built-in potential which is more than 2.1 eV ($\Delta E_{\text{total}} = \Delta E_{\text{barrier}} + E_{\text{bi}}$). This large hole barrier prevents the injection of holes into the ZnO and causes the recombination to occur in the Si. Since Si is not a luminescence material and electron–hole pairs cannot recombine within ZnO, this system cannot produce light. After a forward potential is applied (forward potential with respect to the p–n junction), the potential of the Pt ($V1$) becomes higher than the potential of the Si ($V2$). The height of the Schottky barrier is still the same and the current is limited by the metal–semiconductor junction (figure 4(a) $V1 > V2$). When a reversed bias is applied, $V2$ becomes higher than $V1$. The p–n reverse barrier is higher and the current behavior including breakthrough potential will mainly depend on the p–n (Si–ZnO) junction (figure 4(a) $V1 < V2$). Conclusively, the forward current is largely influenced by the Pt–ZnO junction due to the Schottky barrier, and the reverse current represents the characteristic from ZnO–Si as the p–n heterojunction diode. In figure 4(c), the I–V characteristic of the diode is shown. The forward characteristic has a turn-on voltage at 15 V. This high turn-on voltage is a direct effect from the metal–semiconductor junction. The reverse characteristic comes from the p–n junction and the breakthrough has not yet appeared even for 20 V. This high breakthrough potential indicates an encouraging diode property which suggests the possibility of high performance of the nanodevice in the future.

It is important to emphasize that this technique is not bound to ZnO, but can be extended to any material which can be deposited by ALD. It was proven here that the ALD ZnO NWs have good properties which means that the ALD type NWs can be used to substitute other growth processes of NWs. The fabrication method allows several materials which cannot be grown to be fabricated in the form of nanowires, for example Al_2O_3, TiO_2 TiN, TaN, WN, NbN, Pt, or even including magnetic NiO NWs which have potential in memory device application. Hence, many applications can be harvested based on this unique fabrication procedure.

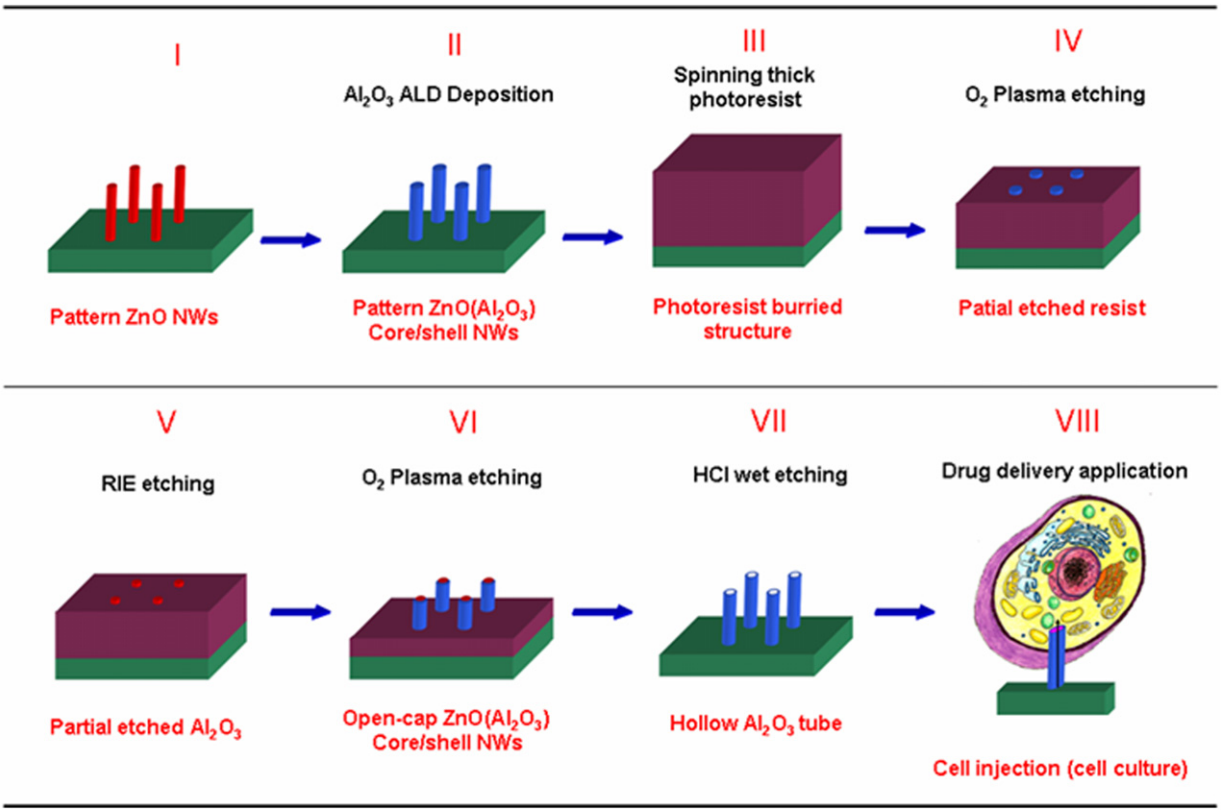

Figure 5. The fabrication process of ALD Al_2O_3 hollow structure.

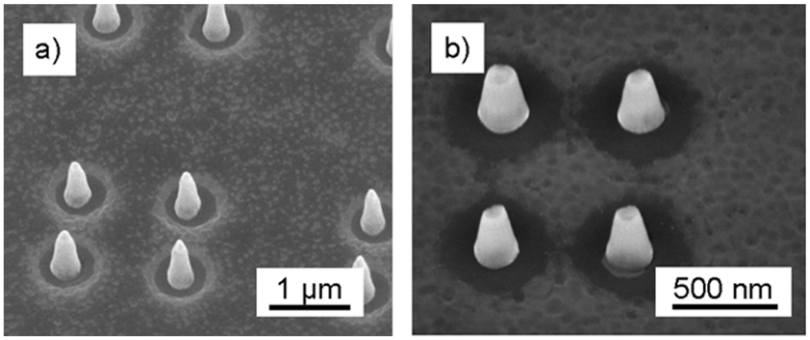

Figure 6. (a) The ZnO/Al_2O_3 core/shell structure which resembles the structure in figure 5 (VI). (b) The Al_2O_3 hollow structure which resembles the structure in figure 5 (VII).

We are now envisioning an additional process as an example for biological application such as cell injection as shown in figure 5. The patterned ZnO NWs were coated with Al_2O_3 and buried in a thick photoresist. The photoresist was partially etched until the tops of the ZnO/Al_2O_3 core/shell NWs appeared. The remnant photoresist acted as the etched mask to protect the other area of the ZnO/Al_2O_3 core/shell structure. The sample was etched by an RIE process and the Al_2O_3 was etched away. The sample was later on washed in high concentration HCl (35% vol.) to dilute the internal ZnO away. After the O_2 plasma etching process, a hollow structure of Al_2O_3 tubes was obtained. In figure 6(a), the ZnO/Al_2O_3 core/shell structure which resembles figure 5(VI) is shown. The internal ZnO part was later on etched away and the hollow Al_2O_3 tube structure is shown in figure 6(b). Since Al_2O_3 is a bio-compatible material, the hollow structure is very promising for biological applications like cell injection [15]. However, the biological experiment was not in the scope of this paper, but can be extended in the near future.

4. Conclusion

A low temperature fabrication method for ZnO NW arrays has been proposed. The size of the ALD ZnO NWs is comparable to the size of ZnO NWs grown by the vapor phase deposition technique. The ALD ZnO NWs are polycrystalline, but the photoluminescence results show an enhanced UV emission and a suppression of the deep level luminescence which indicate that they might be suitable for future optical applications. The ALD ZnO NWs can be used as nanowire diodes as shown by the diode characteristics of selected

wires measured by Pt tips on a nanomanipulator. The result demonstrates encouraging diode characteristics for future nanoelectronic applications. This fabrication method provides the possibility of obtaining vertically arranged ZnO NWs on commercial Si wafer regardless of the incompatibility of the crystal orientation.

References

[1] Heo Y W, Norton D P, Tien L C, Kwon Y, Kang B S, Ren F, Pearton S J and LaRoche J R 2004 *Mater. Sci. Eng.* R **47** 1–47

[2] Zimmler M A, Voss T, Ronning C and Capasso F 2009 *Appl. Phys. Lett.* **94** 241120

[3] Choi A, Kim K, Jung H-I and Lee S Y 2010 *Sensors Actuators* B **148** 577–82

[4] Youn S K, Ramgir N, Wang C, Subannajui K, Cimalla V and Zacharias M 2010 *J. Phys. Chem.* C **114** 10092–100

[5] He Y, Wang J-A, Chen X-B, Zhang W-F, Zeng X-Y and Gu Q-W 2010 *J. Nanopart. Res.* **12** 169–76

[6] Liu J, Goud J, Raj P, Iyer M, Wang Z L and Tummala R R 2008 *Electron. Compon. Technol Conf.* **58** 1317–22

[7] Wongchoosuk C, Subannajui K, Menzel A, Burshtein I, Tamir A, Lifshitz S Y and Zacharias M 2011 *J. Phys. Chem.* C **115** 757–61

[8] Subannajui K, Güder F and Zacharias M 2011 *Nano Lett.* **11** 3513–8

[9] Ra H-W, Choi K-S, Kim J-H, Hahn Y-B and Im Y-H 2008 *Small* **4** 1105–9

[10] Jeong J S and Lee J Y 2010 *Nanotechnology* **21** 475603

[11] Kim J Y, Ko Park S-H, Jeong H Y, Park C, Choi S-Y, Choi J-Y, Han S-H and Yoon T H 2008 *Bull. Korean Chem. Soc.* **29** 727

[12] Krajewski T A, Łuka G, Wachnicki Ł, Guziewicz E, Godlewsk M, Witkowski B, Łukasiewicz M, Łusakowska E, Kowalski B J and Paszkowicz W 2010 *Phys. Status Solidi* c **7** 1550–2

[13] Ning G-H, Zhao X-P, Li J and Zhang C-Q 2006 *Opt. Mater.* **28** 385–90

[14] Krost A, Christen J, Oleynik N, Dadgar A and Deiter S 2004 *Appl. Phys. Lett.* **85** 1496–8

[15] VanDersarl J J, Xu A M and Melosh N A 2011 *Nano Lett.* at press